Artificial Intelligence-Based Controller for Grid-Forming Inverter-Based Generators

Hassan Issa, Vincent Debusschere, Lauric Garbuio, Philippe Lalanda, Nourredine Hadj Said

Artificial Intelligence-Based Controller for Grid-Forming Inverter-Based Generators

Hassan Issa*†, Vincent Debusschere*, Lauric Garbuio*, Philippe Lalanda†, and Nouredine Hadjsaid*‡
*Univ. Grenoble Alpes, CNRS, Grenoble INP, G2ELab, F-38000 Grenoble, France
†Univ. Grenoble Alpes, CNRS, Grenoble INP, LIG, F-38000 Grenoble, France
‡Nanyang Technological University, Singapore 639798, Singapore

***Abstract*—This paper aims at developing artificial intelligence (AI)-based controllers for grid-forming inverter-based generators. The paper illustrates the relevance of the controller on a simplified isolated microgrid. The adopted AI approach relies on supervised learning, thus implying the need for training datasets. Firstly, the case study and the use cases were selected, and the scenarios were defined to create the training datasets from an experimentally validated virtual synchronous generator (VSG) controller. The use cases represent the black-start of the grid-forming inverter and the variation of the load demands as well as its characteristics. Then, the collected datasets were used to train the AI model, which was integrated in the control of a simulated inverter for testing and comparison with the VSG controller on the selected use cases. The proposed AI-based controller ensures the stability of a simplified microgrid, maintaining voltage and frequency at their nominal values. The continuity of supply is guaranteed and robust to changes in loads characteristics. Furthermore, the proposed controller shows fast responses to load variations in addition to high stability during the transitions between loads.**

***Index Terms*—Grid-Forming Control, inverter-based generators, artificial intelligence, neural networks, supervised learning**

I. Introduction

The need for reducing greenhouse gas emissions and diversifying the sources of electricity production lead to high penetration of renewable energy sources (RES) in the power system [1], [2]. The high penetration of RES has introduced distributed generation, which competes with the more centralized power plants. This evolution of power systems creates new challenges to cope with, e.g., stability of the grid due to the intermittent nature of RES [3]. Moreover, distributed generation units are generally relying on inverter-based generators (IBG), increasing the weakness of distribution grids.

Without changing the way grids are operated, the loss of inertia caused by IBG requires building new control strategies to ensure the stability of the power system in this new context. One of the main solutions that can be found in the literature is to reproduce the behavior of rotating synchronous machines with the help of a virtual synchronous generators (VSG) controller, for which a recent good example would be the observer-based current controller from [4]. Simplifications exist, providing only virtual inertia and droop control [5], [6]. Other alternatives do not attempt to reproduce the known behavior in traditional power systems, like the virtual oscillator [7] or the matching control [8]. Those solutions rely on an often complex model-based controller, necessitating precise tuning and sufficient knowledge of the various parameters of the close electrical environment of generating units.

It is also possible to consider data-driven methods of control. In this context, various AI-based solutions have been studied. An artificial neural network (ANN) was designed for the control of a grid-connected rectifier/inverter under disturbance, considering dynamic and power converter switching conditions [9]. An adaptive critic design-based reinforcement learning approach was considered in controlling virtual inertia-based grid-connected inverters [10]. An ANN was designed for tuning the inertia of a VSG [11], and a data-driven optimal control strategy for VSG was tested with deep reinforcement learning approach [12]. Most of those approaches are either considering the case of grid-following inverters, or they only adapt the inputs or part of the controllers. To the best of our knowledge, the control of grid-forming inverters via data-driven methods has not been completely considered.

In this paper, an AI-based controller is proposed to overcome the necessity of modeling and tuning complex model-based controllers, maintain stability, and achieve a fast response to changes in load characteristics. It offers the possibility to be retrained for new case studies either by generating new training datasets or by applying more advanced artificial intelligence methods. The purpose of the proposed controller is to achieve the voltage and frequency control of the grid-forming unit, which is illustrated in a simplified isolated microgrid environment.

The paper is structured as follows: The simplified isolated microgrid; the selected VSG control policy; and the case study, use cases, and scenarios are described in Section II. Section III describes the proposed AI model, its training procedure, and its implementation for simulation. Section IV discusses the obtained results, comparing the AI-based solution with the VSG controller, at the level of the microgrid's frequency, voltage, and the inverter's current for a selection of scenarios. Finally, Section V concludes and states the main perspectives of the work.

This work has been partially supported by MIAI@Grenoble Alpes, (ANR-19-P3IA-0003).

Presented at ISGT 2022 in Novi Sad, Serbia

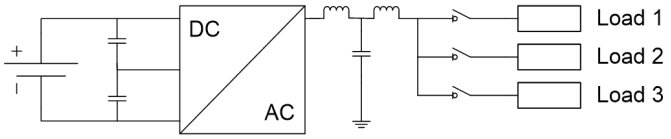

Fig. 1. Simplified Isolated Microgrid, illustration support for the AI controller.

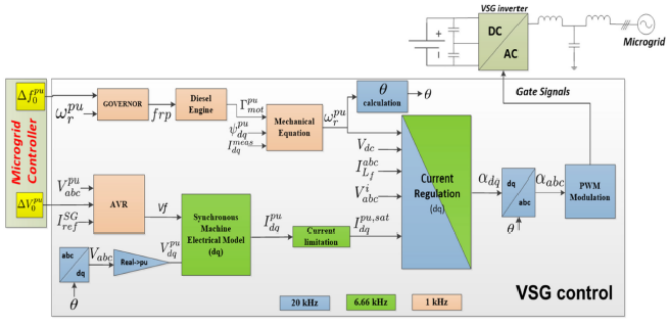

Fig. 2. Diagram of the Virtual Synchronous Generator Controller Used for Data Collection [4].

II. Models and Data Collection

A. Simplified Microgrid Model

The objective is to control a grid-forming unit connected to a simplified isolated microgrid. The IBG is the only generation unit (for instance connected to PV panels via the dc bus). The loads are aggregated at the point of coupling, and they are connected to the IBG through a single line. The simplified balanced three-phase microgrid is operating at the distribution level, i.e., the nominal phase voltage is 230 V and the nominal frequency is 50 Hz. The electrical schematic of the case study is proposed in Fig. 1. For simplification, the dc bus voltage is considered to be constant in this initial study.

The simulation is conducted considering that the IBG is solely supplying power to a single line, connected to three loads with different characteristics presented below. Increasing the size of the microgrid will be considered in further studies, but it is not relevant from the perspective of illustrating the proper behavior of the grid-forming AI-based controller.

B. Classical Control Model

To train the AI-based controller, a dataset is required. Among the various existing grid-forming controllers, the complete VSG controller was preferred [4]. It is a good candidate for initial studies as the model is complete, well-known, and already available from previous work. Indeed, other grid-forming controllers, discussed in the introduction, provide similar behaviors (droop and inertia) or a simplified version, but they require additional implementation steps before data collection for this research. The VSG controller will be compared to other controllers in future work.

The controller consists of a linear quadratic regulator including an integrator and a state observer. It has been designed to ensure high robustness to harsh events (like short-circuits) in addition to load variations of any type. Fig. 2 illustrates the control diagram of the VSG used for data collection.

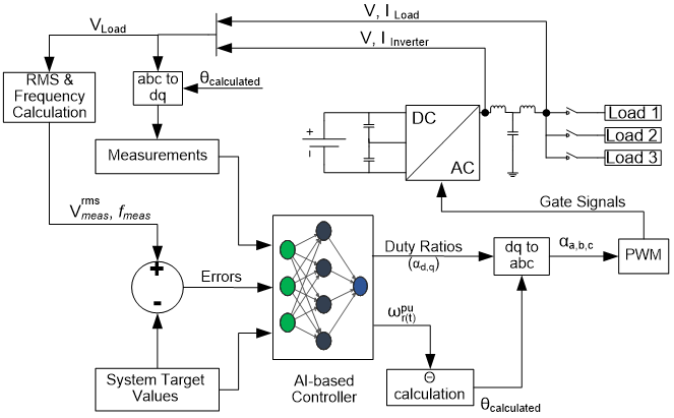

Fig. 3. Implemented Control Policy.

The collected datasets include samples of the expected inputs of the neural network, i.e., frequency; voltages and currents measurements at the output of the inverter and the load after being transformed to the *dq* frame; their associated target values; and computed errors. The corresponding outputs are duty ratios (in *dq*) before being transformed back to *abc* and fed to the pulse width modulation (PWM) block. Moreover, the third output is the angular velocity of the virtual machine's rotor in per unit. The collected datasets are essential for implementing the proposed control policy, shown in Fig. 3.

This control policy may vary in further studies, as a function of case studies, modeling hypotheses, or adjustments needed on the control errors. The AI-based controller is quite flexible in that regard compared to model-based controllers.

C. Case Study, Use Cases, and Scenarios for Data Collection

The case study considered in this paper is the variation of the loads' power demands and characteristics, i.e., capacitive, inductive, and resistive when the solar production is available (no dc-bus voltage variation) and the grid topology is not changing (only one IBG and line). The objective is thus to study the capacity of the proposed AI-based controller to fulfill its goal, which is to ensure the grid-forming operation of the IBG in this context.

As a result, four use cases were introduced to create data, i.e., black-start, resistive, inductive, and capacitive load consumption. The objective is to control the voltages and frequency in the simplified isolated microgrid.

To sufficiently represent the aforementioned use cases, the scenarios for collecting the training datasets were defined in a way that represents a wide range of active and reactive power values. The range considered for active power variations, i.e., resistive loads, is from 0 kW to 15 kW, yet this implies an infinite number of scenarios. Thus, we decided to divide this range into six scenarios, represented by steps of 20 %. The range of reactive power, i.e., negative for capacitive and positive for inductive, is also from 0 kVAR to 15 kVAR, again

with steps of 20 %. The first group of datasets corresponds to the resistive loads (no reactive power consumption). The second group of datasets represents the inductive loads, in which every step of the active power range was simulated with the whole range of positive reactive powers. The third group of datasets includes the capacitive loads, where negative values of reactive power consumption were applied. As a result, 72 datasets were collected to represent the defined scenarios.

The use case of black-start is considered and simulated in each of the 72 generated datasets. The simulation time per scenario was fixed at three seconds. Finally, these 72 datasets were combined in a single dataset for training the AI model. To reduce the rate of necessary and representative data flow in the AI-based controller, the *dq*-frame was considered, as it conserves the required information for efficient operation at a slower rate.

The 16 chosen features, corresponding to the input layer of the neural network, were decided in a way that provides all the necessary information describing the actual situation of the simplified isolated microgrid. The features in the combined training dataset are as follows: voltage and current at the loads (in *dq*-frame), voltage and current at the output of the inverter (in *dq*-frame), frequency of the simplified isolated microgrid, the angular velocity of the virtual machine's rotor at the preceding time step in per unit ($\omega^{pu}_{r_{(t-1)}}$), the target value for the single-phase root mean square (*rms*) voltage (230 V), the target value of the frequency (50 Hz), the errors between measured *rms* voltages and their target ($V^{rms}_{meas} - V^{rms}_{target}$), and the error between the measured frequency and its target ($f_{meas} - f_{target}$). On the other hand, the three chosen labels, corresponding to the outputs of the neural network, are the following: the duty ratios in the *dq*-frame (α_d and α_q) and the angular velocity of the virtual machine's rotor at the actual time step in per unit ($\omega^{pu}_{r_{(t)}}$). From the predicted $\omega^{pu}_{r_{(t)}}$, the electrical angle $\theta_{calculated}$ will be calculated for transforming *abc*-frame to *dq*-frame and vice versa, as shown in Fig. 3.

III. AI Model Training and Implementation

This section describes the proposed AI model, its training procedure, and its implementation for simulation.

Before considering more advanced machine learning techniques, the initial idea is to supervise the training of the model as well as to clearly state what is acceptable or not (in terms of voltage and current) for a dedicated set of use cases. In addition, this phase is considered the initialization of an AI model that will act as a foundation for further developments.

Supervised learning is a technique that learns by using labeled data [13]. The data contain a set of inputs and their corresponding outputs. The term "deep" comes from the several layers between the inputs and the outputs ones. From its definition, the deep supervised learning approach requires the presence of training datasets.

A. Artificial Intelligence Model

The AI model, a sequential feed-forward neural network, interacts with the grid via its input and output layers. The measurements, target values, and errors between measurements and target values are reported to its inputs. The AI model provides the necessary control signals from its output layer by mapping the values reported on its input layer to their corresponding output values. As noted, the expected values on the input layer of the neural network are divided into three categories. The first category, corresponding to the measurements, includes the voltages and currents at the output of the inverter and the load after being transformed to *dq*-frame as well as the frequency. Moreover, the target values category includes the required *rms* phase voltage and the required frequency of the grid. Finally, the category of errors comprehends the differences between the actual measurements collected from the grid (voltages and frequency) and the target values. One the other hand, the duty ratios (in *dq*-frame) and the angular velocity of the virtual machine's rotor (in per unit) are provided by the output layer of the neural network. Thus, the controller will continuously receive new measurements from the grid and provide their corresponding control signals.

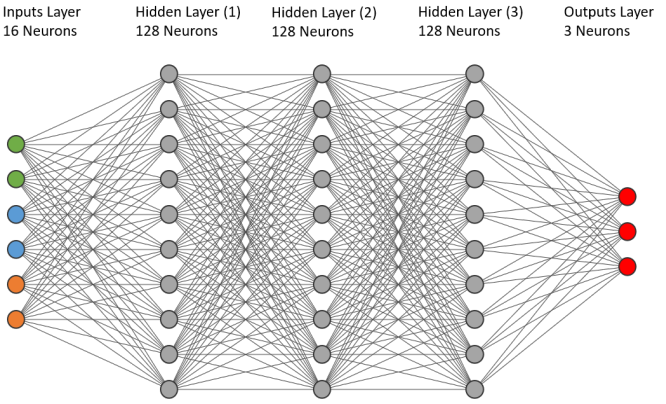

Fig. 4. Implemented Neural Network Architecture.

The architecture of the implemented neural network is described in Fig. 4. As seen, the input layer is composed of 16 artificial neurons corresponding to the previously mentioned three input categories. The neural network includes three dense hidden layers, each composed of 128 artificial neurons. The output layer is made up of three artificial neurons representing the duty ratios (in *dq*-frame) and $\omega^{pu}_{r_{(t)}}$.

Although the input and output layers components were decided concerning the requirements of the controlled system, the hidden layers were defined by testing various combinations of several hidden layers and their components during the training phase. The combination of three hidden layers with 128 artificial neurons each, among the tested ones, has proven the best results and the least errors.

B. Model Training

The proposed feed-forward neural network has been designed and trained using Keras. Keras is a deep learning API that runs on top of TensorFlow, a machine learning platform. Being straightforward, flexible, yet powerful, it has been chosen for the design and training of the AI model.

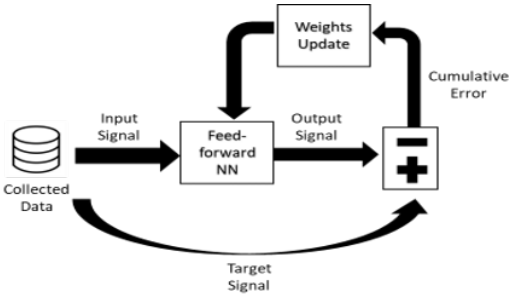

Fig. 5. Training of the Neural Network.

The combined dataset was first shuffled, then divided into two parts: 80 % for training the neural network and the remaining 20 % for the validation. Since the trained neural network is implemented and tested on a simplified microgrid, there is no need for testing datasets. The training phase is graphically illustrated in Fig. 5.

During the training phase, the input signals, i.e., features, are reported to the input layer of the neural network. Then, the neural network provides the output signals, i.e., labels, from its output layer. Later, the predicted values are compared to the actual labels from the combined training dataset, resulting in a cumulative error. The weights of the neural network are updated during the training process concerning the calculated errors between the predicted values and the real values from the training dataset.

The mean absolute error (MAE), whose calculation is used for each epoch of training, is displayed in (1), where n corresponds to the total number of samples in the concerned epoch, y_i corresponds to the i^{th} real label from the training dataset, and x_i corresponds to the i^{th} predicted label.

$$MAE = \frac{1}{n}\sum_{i=1}^{n}|y_i - x_i| \tag{1}$$

Fig. 6 represents the plots of the mean absolute errors during the training phase. The two plots correspond to the MAE of the training part of the dataset as well as the validation part. The training needed less than 30 epochs to reduce the MAE to 0.0003. once the training is completed, the trained model is exported and saved for deployment in the grid-forming unit.

C. Model Implementation

The AI model was developed and trained in Python, while the inverter and the simplified isolated microgrid were implemented in Matlab/Simulink. The interface between the two environments was needed. First, a Python function was coded for importing the AI trained model. Second, a Matlab function was coded for calling the Python function responsible for importing the trained AI model. Then, the Matlab function was integrated as a block in Simulink. As a result, the neural network is implemented directly in Simulink, reproducing the control policy shown in Fig. 3 in the form of an AI-based controller.

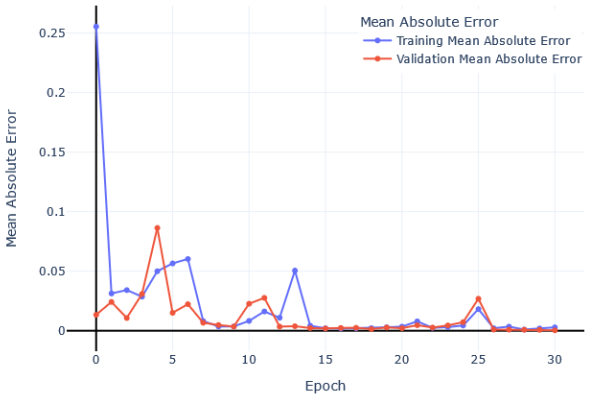

Fig. 6. Mean Absolute Error during Training and Validation.

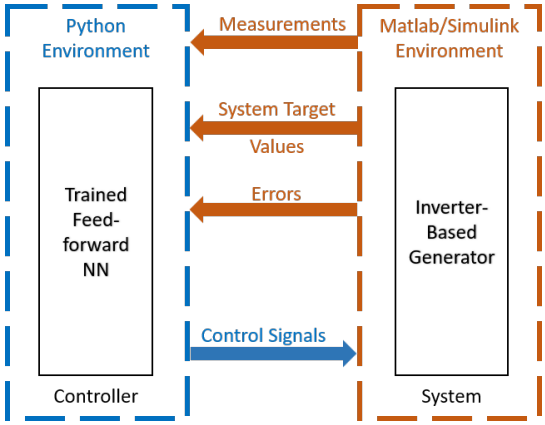

Fig. 7. AI Model Operation and data exchanges between environments.

Fig. 7 graphically describes the methodology of operation and interaction of the AI-based controller with the IBG and its simplified microgrid. The system measurements, target values, and errors are all reported to the input layer of the controller. It then provides the system with the required control signals concerning the values introduced at its input layer.

The AI-based controller's capabilities of conserving the stability of the simplified microgrid (i.e., supply power to the loads in this case) by maintaining the grid voltage and frequency at their nominal values are tested on the defined set of use cases. During testing, only one single load is connected at a time. The changes and characteristics considered in the testing phase are summarized in the tables I and II.

Table I lists the three designed loads' characteristics. *Load 1* is designed to be highly capacitive. *Load 2* is designed to be a relatively small resistive load, corresponding to the microgrid at its lowest demands. Finally, *Load 3* is highly inductive.

Table II lists and describes the events occurring at predefined instants. These simulated events are designed to test the stability and robustness of the proposed AI-based controller under extreme conditions, e.g., transition from a highly capac-

TABLE I
CHARACTERISTICS OF THE CONNECTED LOADS

Load	Active Power (kW)	Inductive Reactive Power (kVAR)	Capacitive Reactive Power (kVAR)
Load 1	15	0	7
Load 2	1	0	0
Load 3	15	7	0

TABLE II
LIST OF OCCURRING EVENTS

Time (s)	Event
0	Black start and connection of *Load 1* only
1	Disconnection of *Load 1* and connection of *Load 2*
2	Disconnection of *Load 2* and connection of *Load 3*

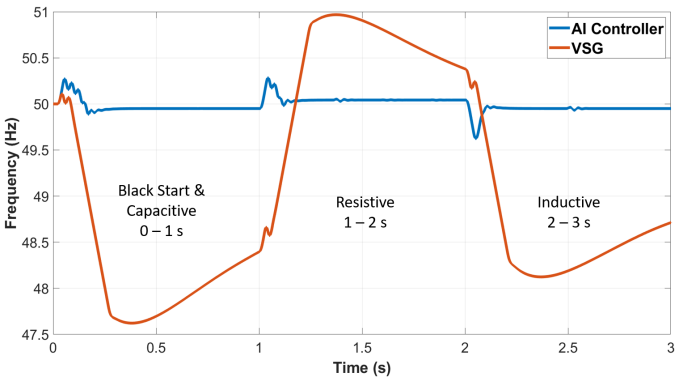

Fig. 8. Frequency Profiles of AI Controller vs VSG, scenarios from Table II.

itive microgrid to a low demand one and later to a microgrid with highly inductive characteristics. Note that the black-start use case is not reproduced directly, but used indirectly for all cases, as all simulations start from zero and are not in a steady state at a given operating point.

IV. OBTAINED RESULTS AND OBSERVATIONS

This section discusses the obtained results based on the scenarios discussed in Table II. Under those conditions, the AI-based controller has been tested and compared to the implementation of the VSG model [4].

A. Frequency and Duty Ratios Profiles

Fig. 8 illustrates the grid's frequency profiles in the cases of the VSG and the AI-based controllers, plotted in orange and blue respectively. By comparing both profiles, we notice that the deviation of the frequency from its nominal value (50 Hz) is minimal in the case of the AI-based controller. Furthermore, it is observed that the VSG was not capable of restoring the frequency at 50 Hz in the considered time frame, while the AI-based controller has almost not deviated from the nominal frequency even after the occurrence of the predefined events.

The positive spike seen in the AI controller's frequency profile, between 0.02 s and 0.15 s, is due to the overshoot in

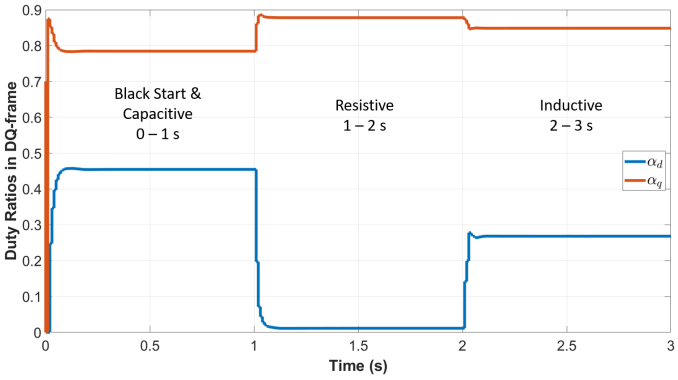

Fig. 9. Duty Ratios (α_d and α_q) of AI Controller, scenarios from Table II.

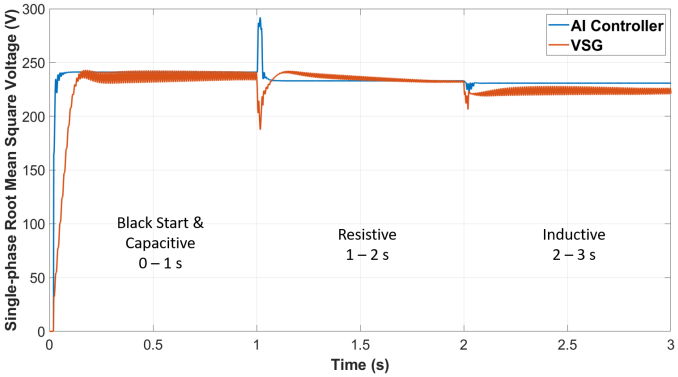

Fig. 10. Single-phase *rms* Microgrid Voltages of AI Controller vs VSG, scenarios from Table II.

the predicted α_d, α_q, and ω_r^{pu}. This limited overshoot occurred following the black-start, yet it was rapidly damped. Fig. 9 illustrates the α_d and α_q profiles.

B. Voltage Profiles

Fig. 10 illustrates the single-phase *rms* voltages (V_{rms}^a) of the simplified microgrid in the cases of both the VSG and the AI-based controllers. Since the three phases are balanced, only one phase (a) was plotted for better visualization. Voltages' deviations from the nominal value (230 V) are strictly limited in the case of the AI-based controller in comparison with the VSG one.

In the case of the AI-based controller, we can notice a spike in the voltage profile at 1 s, rapidly damped. This is due to the small overshoot of α_d seen in Fig. 9. Undesired voltage fluctuations are present for the VSG controller and damped by the AI-based controller. As a result, the proposed AI-based controller shall be more stable and robust in situations of harsh load changes compared to the VSG controller. In addition, the AI controller presents a faster response time, implying faster achievement of the grid's stability, in both black-start and load impacts scenarios.

C. Inverter Current Profiles

Fig. 11 illustrates the single-phase *rms* currents of the inverter in the cases of the VSG and AI-based controllers.

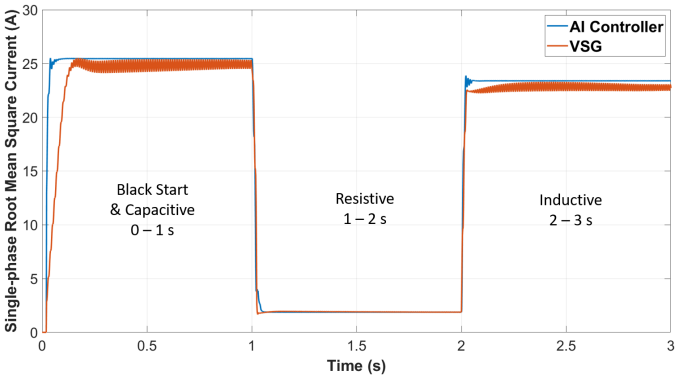

Fig. 11. Single-phase *rms* Inverter Currents of AI Controller vs VSG, scenarios from Table II.

Since the three phases are balanced, only the current in phase a (I^a_{rms}) was plotted for better visualization.

Both controllers are capable of avoiding any current overshoots, specifically during the transition between different microgrid characteristics, thus the inverter is protected and no protection is triggered. Yet after the black-start and during transitions, the current obtained by the AI-based controller achieves its stability faster than the current from the VSG controller. In addition, the current obtained in the VSG case is undergoing undesired fluctuations, notably in the capacitive and inductive cases. In contrast, the current profile of the AI-based controller is subjected to limited fluctuations that are rapidly damped. This implies that the AI-based controller provides a better response to changes and a better power quality.

V. Conclusion and Future Work

In this paper, a supervised deep-learning AI-based controller is trained based on data collected from a simulated virtual synchronous generator (VSG) control. Then, it was implemented in an inverter, reproducing variations in the load demands and characteristics as a case study depicted in more than 70 scenarios. The controller was validated on a set of events with extreme load variations and compared to the actual implementation of the VSG on the same inverter in the case of a simplified microgrid.

The proposed AI-based controller showed a faster and smoother response to changes compared to the VSG one in terms of frequency, voltage, and current profiles, thus providing higher robustness and stability in the cases of harsh load impacts.

The adopted AI method is trained on specific case studies and scenarios, obtained from simulating the VSG control on a typical inverter. As a result, the proposed AI model displays limited adaptability characteristics. Deep reinforcement learning, allowing the AI model to learn its optimal control policy via interacting with its environment represents a clear work path, allowing improved robustness to uncertainty in the renewable production as well as in the grid topology.

References

[1] X. Wang, J. M. Guerrero, F. Blaabjerg, and Z. Chen, "A Review of Power Electronics Based Microgrids," *International Journal of Power Electronics*, vol. 12, no. 1, pp. 181–192, 2012.

[2] Y. W. Li and C.-N. Kao, "An Accurate Power Control Strategy for Power-electronics-interfaced Distributed Generation Units Operating in a Low-voltage Multibus Microgrid," *IEEE Transactions on Power Electronics*, vol. 24, no. 12, pp. 2977–2988, 2009.

[3] T. L. Vandoorn, J. D. M. De Kooning, B. Meersman, and L. Vandevelde, "Review of Primary Control Strategies for Islanded Microgrids with Power-electronic Interfaces," *Renewable and Sustainable Energy Reviews*, vol. 19, pp. 613–628, 2013.

[4] A. Moulichon, M. Alamir, V. Debusschere, L. Garbuio, M. A. Rahmani, M.-X. Wang, and N. Hadjsaid, "Observer-based Current Controller for Virtual Synchronous Generator in Presence of Unknown and Unpredictable Loads," *IEEE Transactions on Power Electronics*, vol. 36, no. 2, pp. 1708–1716, 2020.

[5] L. Subramanian, V. Debusschere, H. B. Gooi, and N. Hadjsaid, "A Cooperative Rate-based Model Predictive Framework for Flexibility Management of DERs," *IEEE Transactions on Energy Conversion*, pp. 2724–2733, 2021.

[6] U. Tamrakar, D. Shrestha, M. Maharjan, B. P. Bhattarai, T. M. Hansen, and R. Tonkoski, "Virtual Inertia: Current Trends and Future Directions," *Applied Sciences*, vol. 7, no. 7, pp. 654–660, 2017.

[7] S. V. Dhople, B. B. Johnson, and A. O. Hamadeh, "Virtual Oscillator Control for Voltage Source Inverters," in *Annual Allerton Conference on Communication, Control, and Computing (Allerton)*, pp. 1359–1363, IEEE, 2013.

[8] C. Arghir, T. Jouini, and F. Dörfler, "Grid-forming control for power converters based on matching of synchronous machines," *Automatica*, vol. 95, pp. 273–282, 2018.

[9] S. Li, M. Fairbank, C. Johnson, D. C. Wunsch, E. Alonso, and J. L. Proao, "Artificial Neural Networks for Control of a Grid-connected Rectifier/Inverter under Disturbance, Dynamic and Power Converter Switching Conditions," *IEEE Transactions on Neural Networks and Learning Systems*, vol. 25, no. 4, pp. 738–750, 2013.

[10] S. Saadatmand, P. Shamsi, and M. Ferdowsi, "Adaptive Critic Design-based Reinforcement Learning Approach in Controlling Virtual Inertia-based Grid-connected Inverters," *International Journal of Electrical Power & Energy Systems*, vol. 127, p. 106657, 2021.

[11] F. Yao, J. Zhao, X. Li, L. Mao, and K. Qu, "RBF Neural Network Based Virtual Synchronous Generator Control With Improved Frequency Stability," *IEEE Transactions on Industrial Informatics*, vol. 17, no. 6, pp. 4014–4024, 2020.

[12] Y. Li, W. Gao, S. Huang, R. Wang, W. Yan, V. Gevorgian, and D. W. Gao, "Data-driven Optimal Control Strategy for Virtual Synchronous Generator Via Deep Reinforcement Learning Approach," *Journal of Modern Power Systems and Clean Energy*, vol. 9, no. 4, pp. 919–929, 2021.

[13] M. Z. Alom, T. M. Taha, C. Yakopcic, S. Westberg, P. Sidike, M. S. Nasrin, M. Hasan, B. C. Van Essen, A. A. S. Awwal, and V. K. Asari, "A State-of-the-art Survey on Deep Learning Theory and Architectures," *Electronics*, vol. 8, no. 3, p. 292, 2019.